

# Spatial distribution and health risk assessment of toxic metals associated with receptor population density in street dust: a case study of Xiandao District, Changsha, Middle China

Fei Li · Jinhui Huang · Guangming Zeng · Xiaolong Huang ·  
Wenchu Liu · Haipeng Wu · Yujie Yuan · Xiaoxiao He · Mingyong Lai

Received: 31 July 2014 / Accepted: 20 October 2014 / Published online: 26 November 2014  
© Springer-Verlag Berlin Heidelberg 2014

**Abstract** Spatial characteristics of the properties (dust organic material and pH), concentrations, and enrichment levels of toxic metals (Ni, Hg, Mn and As) in street dust from Xiandao District (Middle China) were investigated. Method of incorporating receptor population density into noncarcinogenic health risk assessment based on local land use map and geostatistics was developed to identify their priority pollutants/regions of concern. Mean enrichment factors of studied metals decreased in the order of  $Hg \approx As > Mn > Ni$ . For noncarcinogenic effects, the exposure pathway which resulted in the highest levels of exposure risk for children and adults was ingestion except Hg (inhalation of vapors), followed by dermal contact and inhalation. Hazard indexes (*HI*s) for As, Hg, Mn, and Ni to children and adults revealed the following order:  $As > Hg > Mn > Ni$ . Mean *HI* for As exceeded safe level (1) for children, and the maximum *HI* (0.99) for Hg was most approached the safe level. Priority regions of concern were indentified in A region at each residential population density and the areas of B at high and moderate residential population density for As and the high residential density area within A region for Hg, respectively. The developed method was proved useful due to its improvement on previous study for making the priority areas of

environmental management spatially hierarchical and thus reducing the probability of excessive environmental management.

**Keywords** Street dust · Metals · Health risk assessment · Geostatistics · Receptor population density

## Introduction

As a focus of resource consumption and chemical emissions, cities face a variety of problems including public health risk, ecosystem degradation, biodiversity decrease, and so on. Street dust, which consists of soil, deposited airborne particulates, construction material, and soot and fume discharged from the industry and vehicles, etc., is a sensitive indicator of urban environmental quality than single compartmental monitoring of air, water, and soil for it reflects pollutants from the multimedia (Pandey et al. 2014). Further, street dust often contains high levels of toxic metals and organic contaminants such as polycyclic aromatic hydrocarbons (Jiang et al. 2014). Toxic metal contaminations in environment have drawn particular attentions due to their property of high toxicity, concealment, persistence, and biological accumulating (Liu et al. 2014b). Hazardous effects to human health, such as lung cancer, hypertension, and cardiovascular diseases, can be caused by toxic metal residues in street dust via direct inhalation, ingestion, and dermal contact absorption (Kurt-Karakus 2012; Liu et al. 2014a; Yu et al. 2014).

The toxicity and mobility of metals in street dust depend on several factors which include not only the total concentration, but also dust properties like pH and organic matter content (Luo et al. 2011; Nyamangara 1998). In recent years, increasing studies on urban dust have been conducted on toxic metal concentrations, distribution, contamination assessment, health

Responsible editor: Philippe Garrigues

F. Li · J. Huang (✉) · G. Zeng · X. Huang · W. Liu · H. Wu ·  
Y. Yuan · X. He · M. Lai  
College of Environmental Science and Engineering, Hunan  
University, Changsha 410082, China  
e-mail: huangjinhui\_59@163.com

G. Zeng  
e-mail: zgming@hnu.edu.cn

F. Li · J. Huang · G. Zeng · X. Huang · W. Liu · H. Wu · Y. Yuan ·  
X. He · M. Lai  
Key Laboratory of Environmental Biology and Pollution Control  
(Hunan University), Ministry of Education, Changsha 410082, China

risk assessment, and source identification due to its important influence on urban environment quality and human health (Chen et al. 2014; Li et al. 2013; Liu et al. 2014a; Lu et al. 2010; Zhang et al. 2013). Therefore, it is of importance to study in a full-scale consideration about not only the total concentrations of studied metals but also their correlation with dust physicochemical properties spatially. Besides, according to the lots of regional health risk assessment in published reports (Kurt-Karakus 2012; Li et al. 2013; Yu et al. 2014), their results are often of less practical significance for overlooking the principle of “no receptor exposure, no health risk,” and therefore, to make the calculated health risk results connected with corresponding receptor population distribution with different exposure possibilities is significant for helping risk managers to efficiently target limited resources to where they are most required.

In recent three decades, unprecedented economy development in China causes the worldwide attention, and its rapid urbanization tremendously increases the population density and lots of human activities such as traffic, industry, commerce, petrol combustion, and so on. Consequent urban environmental pollution has become an obvious issue related to urban economic stability, human safety, and even social equity (Wei and Yang 2010). Xiandao District (XDD), the pilot district of constructing an environmentally friendly society, belongs to Changsha city which is the capital city of Hunan province, China. XDD has experienced rapid urbanization and industrialization in recent 10 years, which exert a heavy pressure on its urban environment. Therefore, it is of importance to study the spatial pollution patterns, induced health risk distributions of toxic metals in street dust, and to identify detailed priority pollutants/regions of concern in XDD. The objectives of this study were (i) to investigate spatial distribution and correlation of dust properties and toxic metals (Ni, Hg, Mn, and As) in street dust from XDD using contour maps based on geostatistics method of the inverse distance weighted (IDW) interpolation; (ii) to evaluate the enrichment degree of studied metals by their local background values and the enrichment factor (*EF*); (iii) to identify the detailed priority pollutants/regions of concern using the developed method of incorporating receptor population density into noncarcinogenic health risk assessment.

## Materials and methods

### Study area

XDD is a municipal district with a population of over 3 million. The area of XDD is totally 1,200 km<sup>2</sup>, and the urban residents

per capita disposable income reach 3,449 dollar. XDD belongs to subtropical monsoon climate, and its annual average temperature is 17.2 °C. The urban average annual rainfall is 1,361.6 mm. From 2007 to 2013, the urbanization rate in Changsha city rapidly increased from 56.5 to 70.6 %. The local vehicular fleet has increased rapidly in recent years with an annual rate of over 17 % and may reach 2 million vehicles in 2015. Besides, outdoor air quality of Changsha city was not up to Chinese standard level in 168 days out of the whole year 2013. Obviously, rapid urbanization and economic development in XDD have resulted in a decline of its environmental quality (Chen et al. 2011; Li et al. 2007; Yang et al. 2012)

### Sample collection, preparation, and analytical methods

Present land use mapping was determined from a remote-sensing image of the study area. Landsat 7 images acquired on January 15–23 in 2014 were as the source for this work. The original images were successively processed by geometric correction (image to image), image fusion, radiometric calibration, atmosphere correction (FLAASH), and supervised classification using the remote-sensing software ENVI 4.7 (ITT Visual Information Solutions Inc.). Based on the land use map in 2011 and the land use planning map in 2013 of XDD made by the Hunan government, the study area was divided into the detailed land use types based on their remote-sensing spectral characteristics. The processed land use map is shown in Fig. 1.

A total of 51 samples (three parallel samples for each sampling site) were collected around the main streets throughout XDD (Fig. 1). Samples in each sampling site were collected in October 2013 by gently sweeping an area of about 2 m<sup>2</sup> adjacent to the curb of the street with a clean plastic dustpan and brush and transferring about 300 g dust to a polyethylene bag for transport to the laboratory. In the laboratory, all samples were air-dried naturally for 3 weeks, and then sieved through a 100-mesh nylon sieve to remove stones, dead organisms, and coarse debris. The street dust with diameters below 100 µm could be considered to mainly arise from atmospheric deposition and be transported by resuspension (Charlesworth et al. 2011; Zhao and Li 2013); therefore, all the samples were sieved through 200-mesh nylon sieve (diameters below 75 µm) for analysis. Afterward, dust pH was determined with a dust/water ratio of 1:2.5 (*w/v*) using HI 3221 pH meter (Hanna Instruments Inc., USA). Dust organic material (DOM) was determined by oil bath-K<sub>2</sub>Cr<sub>2</sub>O<sub>7</sub> titration method (Nelson and Sommers 1982). For the total metal content detection, 0.40 g samples were picked by an electronic balance (Sartorius TE124S, Germany). Subsequently, the samples were placed in Teflon tubes and digested with

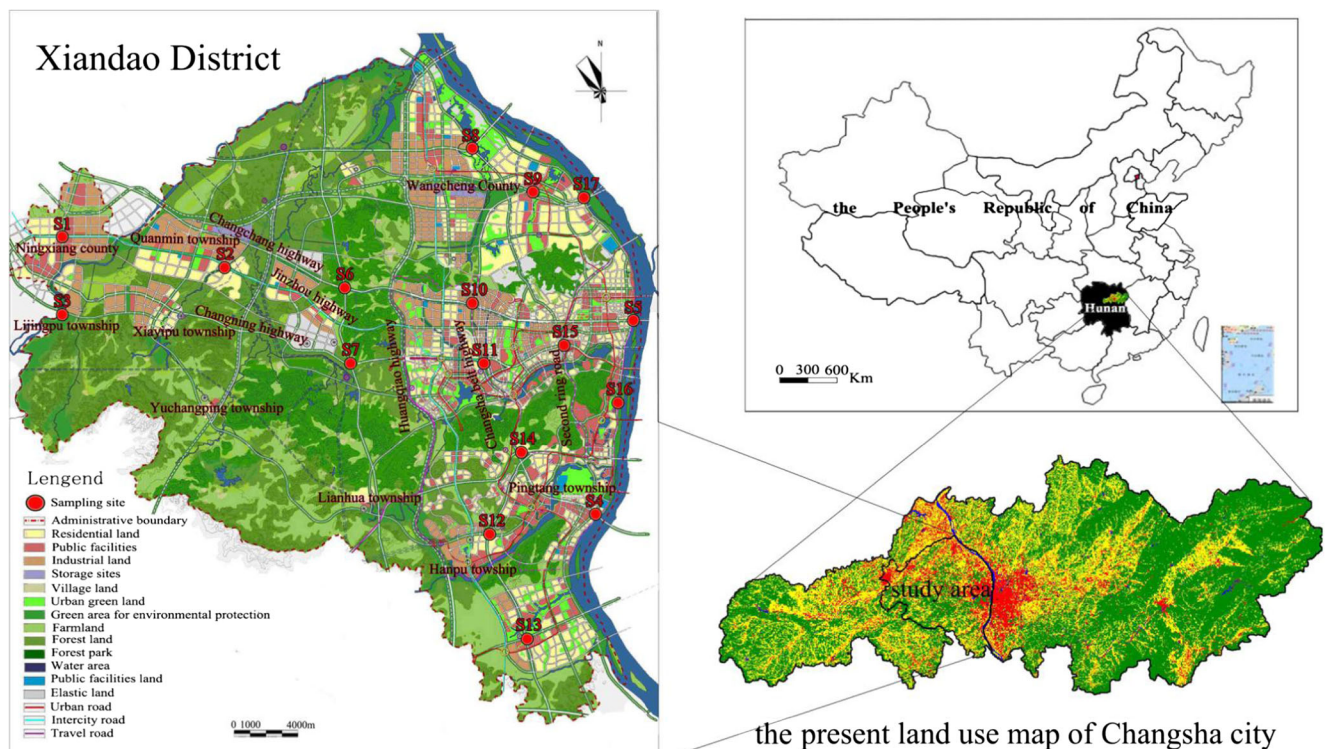


**Fig. 1** Sampling sites in Xiandao District. The right images are the map of China and the present land use map of Changsha city; the left image is detailed map in which different functional zones and urban streets are labeled

HCl,  $\text{HNO}_3$ , HF, and  $\text{HClO}_4$ . Then, the solutions were diluted with 2 % (v/v)  $\text{HNO}_3$  to a final volume of 50 ml and analyzed for Mn, Ni, and Fe by an atomic absorption spectrophotometer (AAAnalyst-700, Perkin-Elmer Inc., USA). Besides, for As and Hg content detection, 10 ml of a freshly prepared mixed acid (1 ml high-concentration  $\text{HNO}_3$ /1 ml high-concentration HCl) was added. The bottle was then covered and the contents mixed. The volumetric flask was then uncovered and placed in boiling water for 2 h, shaking every 30 min. After cooling, 5 ml of 5 % thiocarbamide–5 % ascorbic acid solution was added, and the solution was diluted to 50 ml. Hg was determined in 5 % (v/v) HCl with 20 g/l sodium borohydride ( $\text{NaBH}_4$ ) as the reducing agent; at the same time, the blank and standard substances were determined. And, atomic fluorescence spectrometry (AFS-9700, Haiguang Instruments Inc., China) was used to analyze the concentrations of Hg and As. All other chemicals were of analytical grade. Deionized water was used exclusively for sample preparation. All glass containers utilized in the experiments were soaked in 5 % (v/v) nitric acid for at least 24 h and then rinsed with deionized water to ensure that there was no cross-contamination.

Quality assurance and quality control were assessed using duplicates, method blanks, and state first-level standard materials (GBW GSS-5), with each batch of samples. The analysis

results were reliable when repeat sample analysis error was below 5 % and the analytical precision for replicate samples was within  $\pm 10$  %. Thus, the results met the accuracy demand of the Chinese Technical Specification for Soil Environmental Monitoring HJ/T 166-2004.

#### Pollution and enrichment assessment methodology

An *EF* approach was widely utilized to assess anthropogenic impact of metal pollution on environmental media (Liu et al. 2014a; Zoller et al. 1974). The formula to calculate *EF* was defined as

$$EF = (X_i/R)_{\text{dust}} / (X_i/R)_{\text{background}} \quad (1)$$

where  $(X_i/R)_{\text{dust}}$  and  $(X_i/R)_{\text{background}}$  are the concentration ratios of metal *i* and the normalizer in street dust and background material (Fe in this study), respectively. Elements, such as Fe (Kükrer et al. 2014) and Al (Bourennane et al. 2010; Cesari et al. 2012), were most common references when calculating the *EF* of environmental toxic metal pollutants because they were commonly affected only slightly or remained unaffected in soils, water body sediment, and street dust. Degree of toxic element pollution may be classified into five categories (Sutherland 2000): (1)  $EF < 2$ , minimal enrichment; (2)  $2 \leq EF < 5$ , moderate enrichment; (3)  $5 \leq EF < 20$ ,



significant enrichment; (4)  $20 \leq EF < 40$ , very high enrichment; (5)  $EF \geq 40$ , extremely high enrichment.

## Health risk assessment model

### Exposure evaluation

The models used in present research to evaluate exposure risk of adults or children to toxic metals in street dust are based on models according to US Environmental Protection Agency (USEPA 1996, 2001), the Dutch National Institute of Public Health Agency (Van den Berg 1995), and Technical Guidelines for Risk Assessment of Contaminated Site HJ 25.3-2014 (MEPPRC 2014). The aim receptors mainly including local resident adults or children are exposed through following main pathways: (a) direct ingestion of dust ( $D_{ing}$ ), (b) inhalation of dust particles through mouth and nose ( $D_{inh}$ ), and (c) dermal contact absorption ( $D_{der}$ ), or through inhalation of vapors ( $D_{vap}$ ). The corresponding dose received through each of the exposure paths was evaluated by Eqs. (2)–(5) for noncarcinogenic risk (USEPA 1996, 2001):

$$D_{ing} = \frac{C \times R_{ing} \times EXF \times ED}{BW \times AT} \times 10^{-6} \quad (2)$$

$$D_{inh} = \frac{C \times R_{inh} \times EXF \times ED}{PEF \times BW \times AT} \quad (3)$$

$$D_{der} = \frac{C \times SA \times SL \times ABS \times EXF \times ED}{BW \times AT} \times 10^{-6} \quad (4)$$

$$D_{vap} = \frac{C \times R_{inh} \times EXF \times ED}{VF \times BW \times AT} \quad (5)$$

where  $C$  is the concentration of trace element in street dust, mg/kg;  $R_{ing}$ , the ingestion rate, was estimated to be 200 mg/day for children, 100 mg/day for adults;  $R_{inh}$ , the inhalation rate, was estimated to be 7.6 m<sup>3</sup>/day for children, 20 m<sup>3</sup>/day for adults;  $EXF$ , the exposure frequency, in this study, 350 day/a;  $ED$  is the exposure duration, 6 years for children, 24 years for adults;  $SA$  is the exposed skin area, in this study, 2,448 cm<sup>2</sup> for children, 5,075 cm<sup>2</sup> for adults;  $SL$  is the skin adherence factor, 0.07 mg/m<sup>2</sup>/day for children, 0.2 mg/cm<sup>2</sup>/day for adults;  $ABS$  is dermal absorption factor (unitless), 0.03 for As, 0.001 for other studied metals;  $PEF$  is particle emission factor, in this study, 1.36E+09 m<sup>3</sup>/kg;  $VF$  is

volatilization factor, for Hg, 32,675 m<sup>3</sup>/kg;  $AT$  is the average contact time,  $ED \times 365$  days for noncarcinogens;  $BW$  is the average bodyweight, in this study, 15.9 kg for children, 56.8 kg for adults. All the parameters refer to these literatures (Van den Berg 1995; USEPA 1996, 2001; MEPPRC 2014), and in order to decrease this parameter uncertainty, the local parameters including  $BW$ ,  $SA$ ,  $EXF$ ,  $ED$ ,  $SL$ , and  $AT$  were adopted preferentially (MEPPRC 2014). The following assumptions that underlie the model applied in XDD need to be declared: (1) Intake rates and particle emission and volatilization factors for street dust can be approximated by those developed for soil; (2) biometric and exposure parameters of children or adults in middle China are partly similar to those of a US or Dutch children.

### Risk characterization

Based on calculation of exposure dose at possible exposure pathways, a hazard quotient ( $HQ$ ) for each metal and for each exposure pathway and hazard index ( $HI$ ) which represent the magnitude of adverse effect with total exposure pathways were yielded as follows:

$$HI = HQ_{ing} + HQ_{inh} + HQ_{der} + HQ_{vap} = (D_{ing}/RfD_{ing}) + (D_{inh}/RfD_{inh}) + (D_{der}/RfD_{der}) + (D_{vap}/RfD_{vap}) \quad (6)$$

where  $RfD$  is corresponding reference doses for each toxic metals and for different exposure pathways.  $HI$  is presented as the sum of  $HQ$  for each metal, and noncarcinogenic risk is accepted when the  $HI$  value is below 1 and the degree of risk increases as  $HI$  increases (USEPA 2001; MEPPRC 2014). The reference dose ( $RfD$ ) values of studied metals are shown in Table 3 which were taken from the US Department of Energy's Risk Assessment Information System (RAIS) compilation (US Department of Energy 2014).

### Statistics and geostatistical methods

To explore the relationship between metal concentration and dust properties, the statistical analysis was performed by the software package SPSS version 16.0. And, to make the calculated data visualization spatially, geostatistical method was employed by ArcGIS 9.3. Geographic information system (GIS) was used to spatially analyze the distribution, enrichment level, and induced health risk of metals in street dust from XDD. The IDW method was applied to map the spatial characteristics of pollutants based on the ArcGIS 9.3 software. IDW employs a specific number of nearest points that are then weighted according to their distance from the point being interpolated. In this study, the power of 2 and the number of

neighboring samples of 15 were chosen to clearly show both spatial variation and patterns of the pollutants.

## Results and discussion

### Properties and metal concentrations in street dust

The descriptive statistics of dust properties and metal concentrations in street dust are shown in Table 1, as well as the background values in Hunan province and the guideline values of the Chinese Environmental Quality Standard for Soils. The dust properties covered a wide range of values in pH (8.12–11.33, alkaline state) and DOM (0.25–12.58 %). pH and dust organic matter may influence chemical speciation transformations and the absorption of metals in dust and soil. Application of the Shapiro–Wilk test confirmed that the detected data of As, Hg, Ni, and pH were normal distribution ( $\text{sig.} > 0.05$ ), whereas other metals and DOM were nonnormal distribution. Therefore, log-transformation was utilized, and the distribution of Mn, Fe, and DOM conformed to normal distribution after log-transformation, namely, they conformed to logarithmic normal distribution. Arithmetic mean and geometric mean are the mathematical expectation of normal distribution and logarithmic normal distribution, respectively. The ranges and arithmetic or geometric mean concentrations

of studied metals in street dust were As 4.47–60.20 (24.47) mg/kg, Hg 0.09–0.23 (0.15) mg/kg, Mn 419–1,856 (764) mg/kg, Ni 9.20–64.60 (30.74) mg/kg, and Fe 1.12–4.54 (2.15) %. The mean concentrations of As, Hg, Mn, and Ni were higher than their corresponding background values in Hunan province soils at 1.63, 1.67, 1.73, and 1.71 times, respectively. High coefficients of variation ( $\text{CV} = 100\text{SD}/\text{Mean}$ ) were found for As, Mn, and Ni indicating their high inhomogeneity which probably be effected by human activities. Compared with the values of the Chinese Environmental Quality Standard for Soils, As was generally higher than class III of National Soil Standards. Hg and Ni were mainly lower than class II of National Soil Standards with 0 and 5.9 % of sites were higher than class II of National Soil Standards.

Comparison of the street dust metal data in XDD of Changsha city with the published data in street dust from different cities at home and abroad (Table 2), it revealed that As in the road dust from XDD was in relatively higher pollution degree which accorded with that in Beijing street dust. Besides, Hg and Mn were in relatively moderate concentration degree. Detailed comparisons are clearly presented in Table 2.

### Spatial distribution of metals and their enrichment factors

The spatial distribution of studied metals and dust properties is very useful to identify the possible sources of enrichment and to preliminarily screen hot spot areas with high metal pollution (Chen et al. 2014; Li et al. 2013; Liu et al. 2014a). Based on the concentrations of studied metals in street dust from XDD and IDW interpolation method, their spatial distribution maps are shown in Fig. 2 and Fig. 3.

Spatial distribution of As (Fig. 2a), compared with spatial distributions of other metals, was in special distribution. Average concentrations of As from each sampling site decreased in the order of  $\text{S14} > \text{S3} > \text{S12} > \text{S7} > \text{S11} > \text{S4} > \text{S2} > \text{S9} > \text{S16} > \text{S8} > \text{S17} > \text{S6} > \text{S1} > \text{S13} > \text{S5} > \text{S15} > \text{S10}$  (Fig. 2a). The lower northwest corner and southeast parts of XDD were the parts of higher concentration.

According to Fig. 2b and Fig. 3e, the distributions of DOM and Hg were similar to some extent. Average concentrations of Hg from each sampling site decreased in the order of  $\text{S7} > \text{S1} > \text{S6} > \text{S2} > \text{S12} > \text{S15} > \text{S11} > \text{S14} > \text{S9} > \text{S3} > \text{S16} > \text{S4} > \text{S5} > \text{S8} > \text{S17} > \text{S13} > \text{S10}$ . The upper northwest corner and middle parts of XDD were in higher concentration.

Based on Fig. 3c, g, there were partly similar spatial distributions between Ni and pH in XDD. With regard to Ni, average concentrations from each sampling site decreased in the order of  $\text{S15} > \text{S2} > \text{S6} > \text{S12} > \text{S16} > \text{S13} > \text{S10} > \text{S1} > \text{S7} > \text{S4} > \text{S9} > \text{S11} > \text{S14} > \text{S5} > \text{S3} > \text{S8} > \text{S17}$  (Fig. 3c). Spatially, the middle east parts of XDD were of higher concentration.

Distribution of Mn and Fe also shows partly similar spatial distributions (Fig. 3d, f). Average concentrations of Mn from

**Table 1** Descriptive statistics of studied metal concentrations and dust properties in street dust from Xiandao District mg/kg

Elements	As	Hg	Mn	Ni	Fe	DOM	pH
					(%)	(%)	
Max	60.20	0.23	1856	64.60	4.54	12.58	11.33
Min	4.47	0.09	419	9.20	1.12	0.25	8.12
AM	24.47	0.15	824	30.74	2.26	3.00	9.43
GM	18.88	0.14	764	28.27	2.15	1.86	9.40
SD	16.87	0.04	360	12.48	0.80	0.03	0.84
CV(%)	68.94	26.67	43.65	40.60	35.30	1.00	8.91
S-W Sig.	0.119	0.124	0.012	0.245	0.018	0.018	0.147
BV <sub>China</sub> <sup>a</sup>	11.20	0.07	533	26.90	2.94	2.54	4.80
BV <sub>Hunan</sub> <sup>b</sup>	15.00	0.09	441	18.00	NA	NA	NA
Calss I <sup>c</sup>	15	0.15	NA	40	NA	NA	NA
Calss II <sup>c</sup>	25	1.0	NA	60	NA	NA	NA
Calss III <sup>c</sup>	40	1.5	NA	200	NA	NA	NA

<sup>a</sup> CNEMC (China National Environmental Monitoring Center) (1990)

<sup>b</sup> Soil background values of Hunan province, China (Pan and Yang 1988; Zhou et al. 2008)

<sup>c</sup> Environmental quality standard secondary grade for soils, soil limitations to ensure agricultural production, and human health (National Environmental Protection Agency of China 1995)

GM geometric mean, SD standard deviation, CV coefficient of variation, AM arithmetic mean; S-W Sig. significance based on Shapiro–Wilk test, NA not available.

**Table 2** Summaries of studied metals in street dust from different cities at home and abroad mg/kg

Sites	As	Hg	Mn	Ni	
Nanjing (China)	13.4	0.12	NA	55.9	(Hu et al. 2011)
Xi'an (China)	13.2	NA	558.3	34.6	(Chen et al. 2014)
Baoji (China)	19.8	1.11	804.2	48.8	(Lu et al. 2010)
Shanghai (China)	8.01	0.14	NA	66.44	(Shi et al. 2010)
Beijing (China)	23.70	NA	591.44	NA	(Tang et al. 2013)
Luanda (Angola)	5.00	3.4	NA	67.9	(Ferreira-Baptista and De Miguel 2005)
Tehran (Iran)	NA	NA	1214.5	34.8	(Saeedi et al. 2012)
Kavala (Greece)	16.7	0.1	NA	57.5	(Christoforidis and Stamatis 2009)
Alcalá de Henares (Spain)	4.83	NA	99.27	6.56	(Peña-Fernández et al. 2014)
Present study	24.47	0.15	764.19	30.74	

each sampling site decreased in the order of S12>S15>S13>S16>S5>S6>S11>S10>S8>S14>S4>S9>S2>S3>S17>S1>S7. Fe, as the most abundant metal and the fourth most common element in the Earth's crust, was regarded as reference element in calculation of *EFs*. The southeast parts of XDD were the parts of higher concentration.

Combined with the present land use map of XDD in Changsha city (Fig. 1), there was an obvious truth that the spatial distributions of studied metal concentration were in close relationship with probable anthropogenic input. Besides, DOM-Hg, Ni-pH, and Mn-Fe may have close relationship and derive from similar source, respectively.

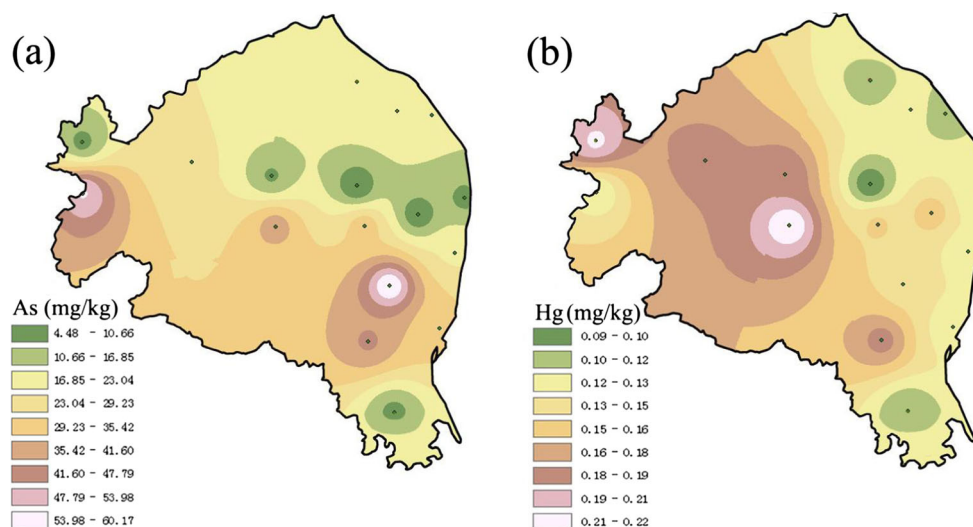
To further quantitatively assess the enrichment degree of studied metals, the spatial *EF* distributions, based on the calculated results by Eq. (1) and IDW interpolation method, are shown in Fig. 4.

According to Fig. 4, mean *EFs* of metals (As, Hg, Mn, and Ni) in street dusts were all above 1. The ranges and arithmetic mean *EFs* of metals in street dust were As 0.58–9.24 (3.30), Hg 1.89–9.19 (3.31), Mn 1.27–3.34 (2.04), and Ni 0.43–3.61

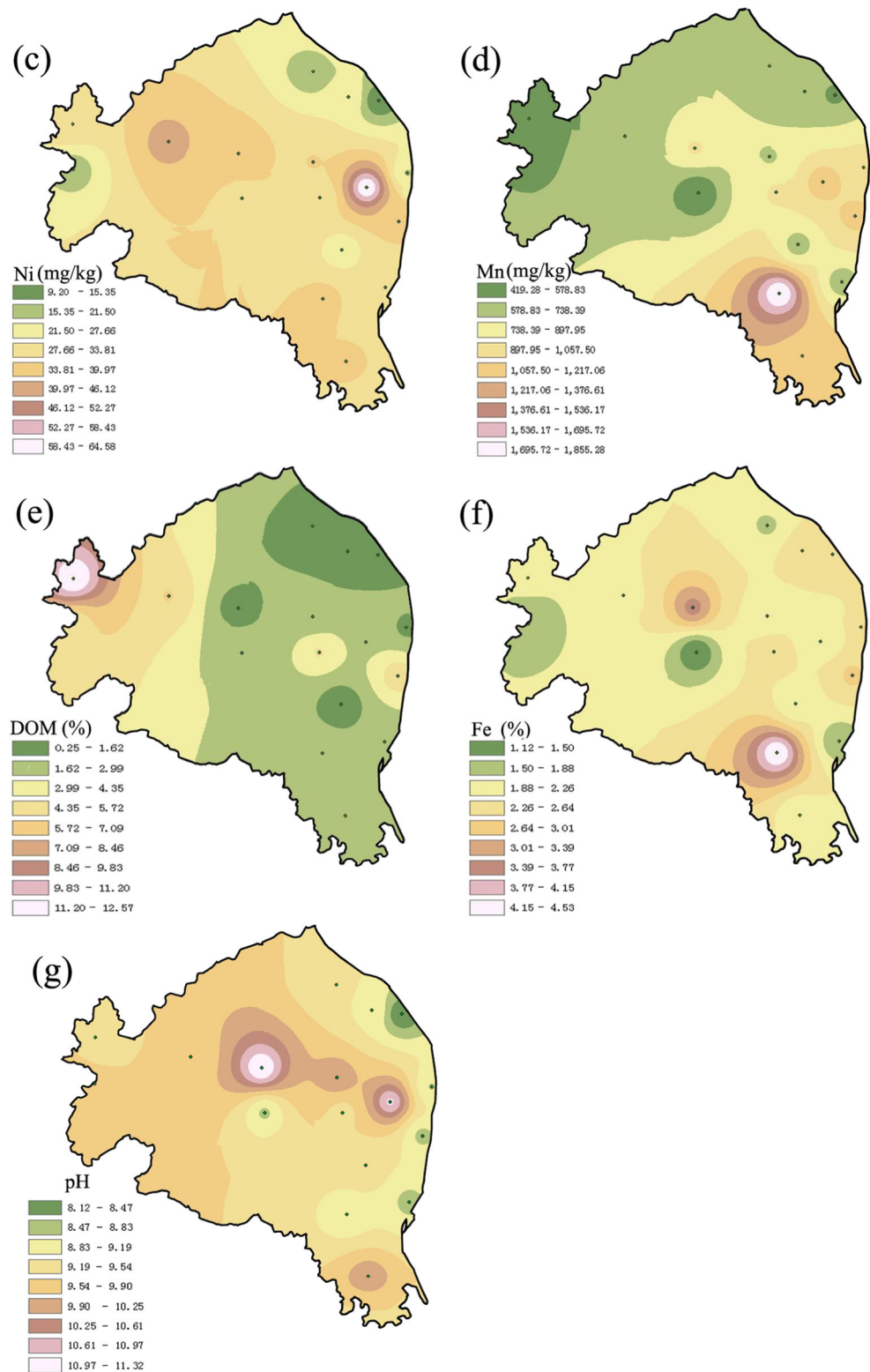
(1.61). The ranking of mean *EF* levels of the metals follows Hg (moderate enrichment)≈As (moderate enrichment)>Mn (moderate enrichment)>Ni (minimal enrichment). Besides, for As, Hg, Mn, and Ni, there were 64.71, 91.11, 47.06, and 23.53 % out of all sampling sites exceeding *EF* value 2 (Fig. 4) and 23.53, 5.88, 0, and 0 % out of all sampling sites exceeding *EF* value 5. In short, As and Hg were in higher enrichment level, and the enrichment distribution of As was in larger spatial variability than that of Hg.

Integrated human health assessment of children and adults to street dust metals

After investigating spatial enrichment of studied metals, non-carcinogenic health risk assessment for adults and children from exposure to metals in street dust from XDD through possible exposure pathways (ingestion, dermal contact, and inhalation) was calculated based on Eqs. (2)–(6), and results are shown in Table 3. The total exposure *HQs* from ingestion, dermal contact, and inhalation for all studied metals in each

**Fig. 2** Spatial distribution of studied metals in street dusts in XDD. **a** As; **b** Hg


**Fig. 3** Spatial distributions of metals and dust properties in street dusts in XDD. **c** Ni; **d** Mn; **e** DOM; **f** Fe; **g** pH



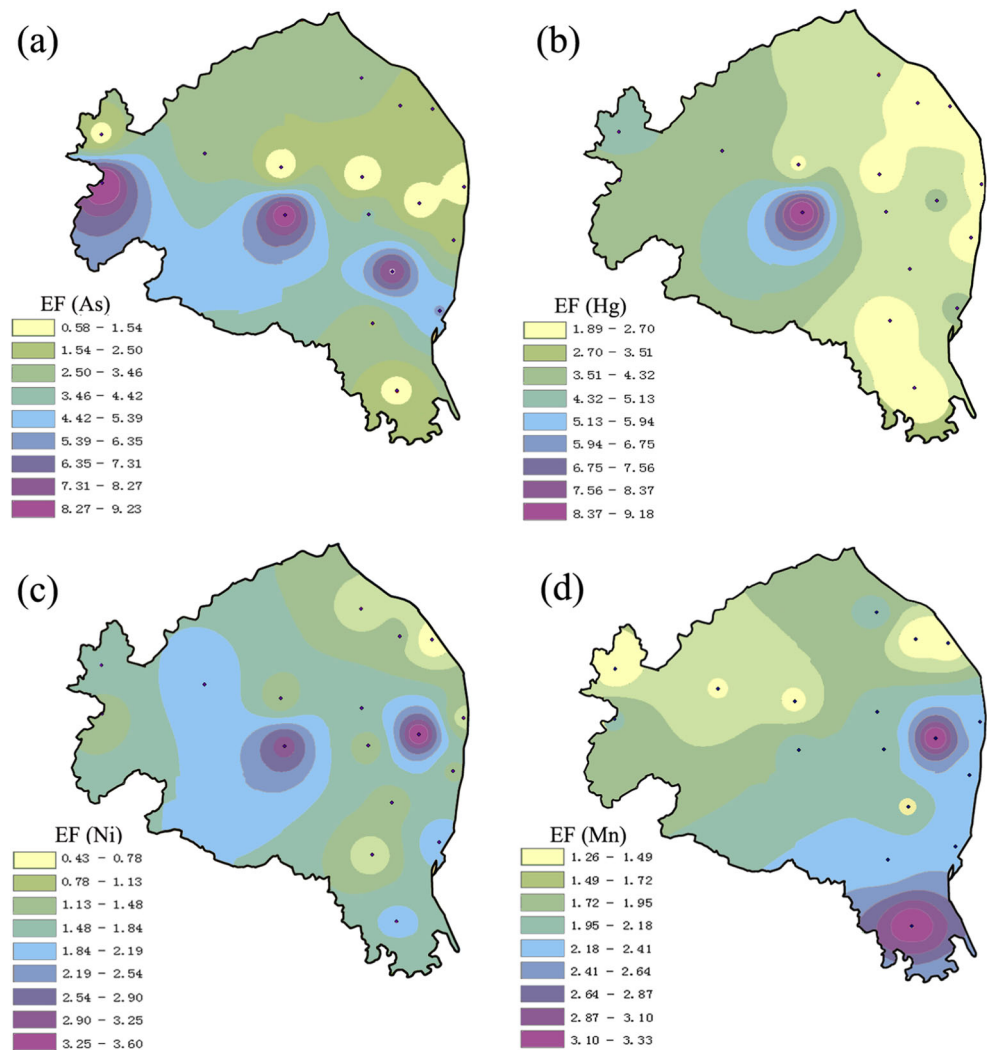
sample were higher for children than those for adults (Table 3).

For noncarcinogenic risk of As, Mn, and Ni, ingestion of dust particles appeared to be the main exposure route for

metals to children and adults, followed by dermal contact and inhalation (Table 3). And, *HQs* of As and Ni due to inhalation of dust particles were much lower than those due to other exposure pathways. And, only for *HQ* of Hg,



**Fig. 4** Spatial EF distribution of studied metals in street dust from Xiandao District. **a** As; **b** Hg; **c** Ni; **d** Mn



inhalation of vapors appeared to pose the highest risk due to significant vapor pressure of Hg at ambient temperature (Zheng et al. 2010), followed by ingestion, dermal contact, and inhalation (Table 3).

Further, *HI*s for Ni, Hg, Mn, and As to children and adults decreased in the order of  $As > Hg > Mn > Ni$ . And, the mean *HI* for As exceeded safe level (1) for children and adults, and the maximum *HI* (0.99) for Hg most approached the safe level in this study (Table 3). Moreover, the mean *HI*s of Hg, Mn, and Ni were all within the safe level, whereas *HI*s of Hg were generally 2 times and 1 order of magnitudes higher than those of Mn and Ni, respectively (Table 3). Contacting by receptors in enough doses of As can affect the gastrointestinal tract, respiratory tract, skin, liver, cardiovascular, hematopoietic, and nervous systems (Al Rmalli et al. 2005). It can also cause blackfoot disease and cancer risks for skin and various viscera, including the lung, bladder, kidney, and liver (Duker et al. 2005; Hughes 2002; Mandal and Suzuki 2002). Hg can damage the nervous system and kidneys and cause Minamata disease (Walcek et al. 2003; Ye et al. 2009). Hence, As

exposure due to street dust from XDD should be regarded as priority pollutant of concern and potential noncarcinogenic risk of Hg cannot be overlooked for children and typically occupational receptors such as taxi drivers and street cleaners who may also be at health risk due to their relatively long-term exposure to the street dust.

To efficiently identify in detail the priority areas and make the corresponding risk management strategy, it is significant to provide the integrated spatial health risk map with the possible exposure information about receptors to decision makers. Under condition that the accurate population distribution was unknown for limited manpower and material resources, processed residential population density map was made out of the detailed land use map due to the close relationship between the population distribution and the local land use pattern. Further, areas of XDD were preliminary divided into four parts including areas of high residential population density (residential land and public facilities included), moderate residential population density (village land and urban green land included), low residential population density (industrial land

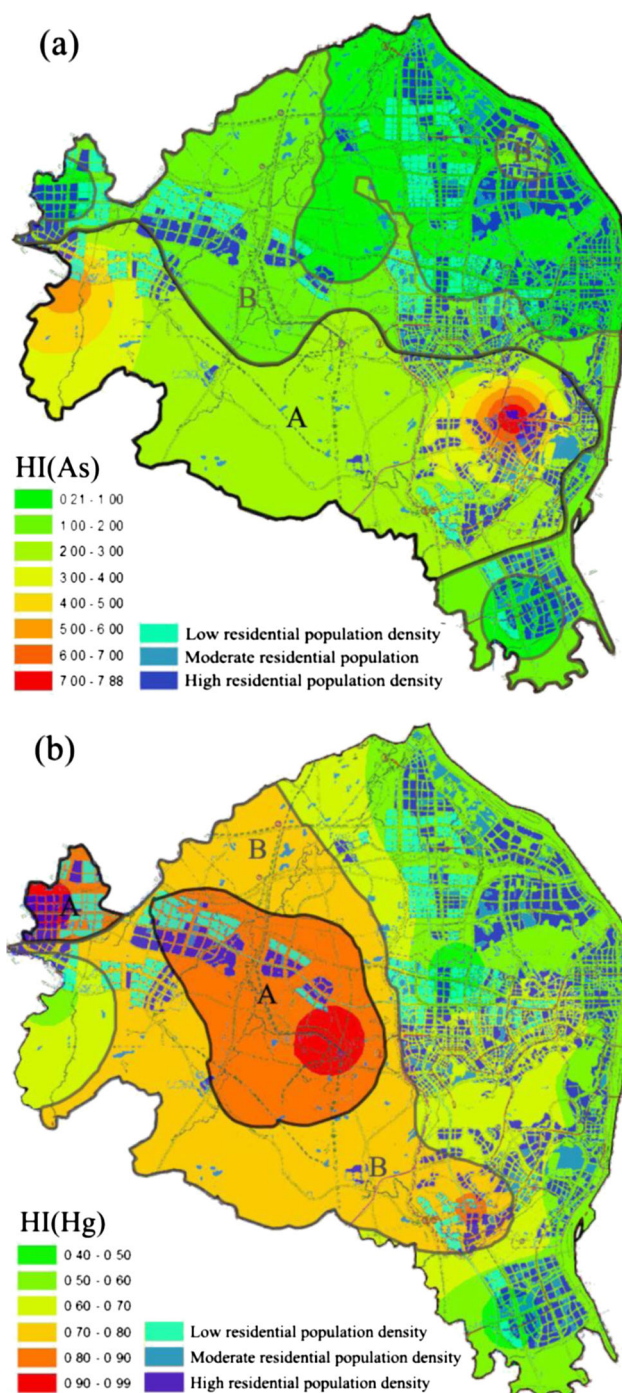


**Table 3** Reference dose and hazard quotient for each metal and exposure pathway

		As	Hg	Mn	Ni
	$RfD_{ing}$	3.00E-04	3.00E-04	4.60E-02	2.00E-02
	$RfD_{dermal}$	1.23E-04	2.10E-05	1.84E-03	5.40E-03
	$RfD_{inh}$	3.01E-04	8.57E-05	1.43E-05	2.06E-02
Children					
$HQ_{ing}$	Min	3.69E-01	3.71E-03	1.10E-01	5.57E-03
	Max	6.69E+00	9.20E-03	4.88E-01	3.91E-02
	Mean	1.46E+00	6.02E-03	2.17E-01	1.86E-02
$HQ_{inh}$	Min	5.00E-06	3.62E-07	9.87E-03	1.51E-07
	Max	1.86E-04	8.97E-07	4.37E-02	1.06E-06
	Mean	4.04E-05	5.87E-07	1.94E-02	5.03E-07
$HQ_{der}$	Min	3.22E-02	1.29E-04	6.72E-03	5.03E-05
	Max	1.19E+00	3.20E-04	2.98E-02	3.53E-04
	Mean	2.60E-01	2.10E-04	1.32E-02	1.68E-04
$HQ_{vap}$	Min	—	3.96E-01	—	—
	Max	—	9.82E-01	—	—
	Mean	—	6.43E-01	—	—
$HI$	Min	2.12E-01	4.00E-01	1.27E-01	5.62E-03
	Max	7.88E+00	9.92E-01	5.62E-01	3.94E-02
	Mean	1.72E+00	6.49E-01	2.49E-01	1.88E-0
Adults					
$HQ_{ing}$	Min	2.52E-02	5.18E-04	1.54E-02	7.77E-04
	Max	9.34E-01	1.28E-03	6.82E-02	5.46E-03
	Mean	2.03E-01	8.40E-04	3.03E-02	2.60E-03
$HQ_{inh}$	Min	3.68E-06	2.66E-07	7.27E-03	1.11E-07
	Max	1.37E-04	6.60E-07	3.22E-02	7.78E-07
	Mean	2.97E-05	4.32E-07	1.43E-02	3.70E-07
$HQ_{der}$	Min	6.54E-03	2.63E-05	1.37E-03	1.02E-05
	Max	2.43E-01	6.51E-05	6.05E-03	7.18E-05
	Mean	5.28E-02	4.26E-05	2.69E-03	3.42E-05
$HQ_{vap}$	Min	—	5.55E-02	—	—
	Max	—	1.37E-01	—	—
	Mean	—	8.99E-02	—	—
$HI$	Min	3.17E-02	5.60E-02	2.40E-02	7.88E-04
	Max	1.18E+00	1.39E-01	1.06E-01	5.53E-03
	Mean	2.56E-01	9.08E-02	4.73E-02	2.63E-03

included), and the rest area with scarce receptor exposure possibility. And, the interpolation maps of the  $HI$ s for As and Hg to children were made with overlay of the processed residential population density map and shown in Fig. 5.

According to Fig. 5a, it showed that above 60 % areas of XDD were under noncarcinogenic health risk for children. And generally, the south area of XDD was under higher  $HI$ s than that of north area. To identify the detailed priority regions of concern for decision maker, the A and B regions were divided based on  $HI$ s of As and Hg, and  $HI$ s (A) >  $HI$ s (B).

**Fig. 5** Interpolation maps of the  $HI$ s for As **a** and Hg **b** with overlay of the processed residential population density map

For As,  $HI$ s of both the regions A and B exceeded safe level (1), and therefore, the areas of A at each population density and the areas of B at high and moderate population density were suggested as priority regions of concern.

According to Fig. 5b, the west area of XDD was under higher  $HI$ s than that of east area generally. And, the hot spots were mainly in the Ningxiang county, west parts of Changjing, Jinzhou, and Changchang highways. For Hg,

*HI*s of both the areas A and B not exceeded but approached safe level (1). In consideration of residential population density, Fig. 5b obviously showed that the high residential density area within A region should be suggested as priority regions of concern for Hg, and the low residential population density area within A region and high residential population density area within B region cannot be overlooked especially for children and corresponding occupational receptors.

The evaluation of uncertainty is an important step accompanying the health risk assessment. Some sources of uncertainty are well emphasized in the literature (Li et al. 2012) and are inherent like the reference toxicity values (Van den Berg 1995; Ferreira-Baptista and De Miguel 2005) and PEF. And, the exposure parameters used to characterize the risks adapt to the people of whole country. Therefore, it is recommended that a clinical toxicological research should be carried out in XDD, and the precise epidemiological consequences on children and adults living in different communities in XDD with exposure to the street dust should be performed. Further, other metals (i.e., Cd, Cr, and Cu) and other potential exposure way (i.e., contaminated soils or indoor dusts) were not considered in this study. Finally, accurately spatial population density and seasonal changes of studied metal concentration were also not considered. However, though there are some uncertainties, the present study would pose a useful tool to assess the human health risk associated with receptor population density and could help to supply detailed and hierarchical information to the public or government about detailed priority pollutants/regions of concern spatially.

## Conclusions

The concentrations of As, Hg, Mn, and Ni in street dusts from XDD were higher than their local soil background values to different extent, indicating an anthropogenic input. The ranking of mean *EF*s of studied metals follows Hg (moderate enrichment)  $\approx$  As (moderate enrichment)  $>$  Mn (moderate enrichment)  $>$  Ni (minimal enrichment). Spatially different distribution patterns were found among the analyzed metals, and there were partly similar distributions among Hg-DOM, Ni-pH, and Fe-Mn which might indicate their correlation and similar sources.

For noncarcinogenic effects, the exposure pathway which resulted in the highest levels of exposure risk for children and adults was ingestion except Hg (inhalation of vapors), followed by dermal contact and inhalation. *HI*s for As, Hg, Mn, and Ni to children and adults decreased in the order of As  $>$  Hg  $>$  Mn  $>$  Ni. As exhibit *HI*s larger than safe level (1) for children and adults, and the maximum *HI* (0.99) for Hg was most approached the safe level. Hence, As exposure due to street dust from XDD should be regarded as priority control factor,

and potential noncarcinogenic risk of Hg cannot be overlooked for children and typically occupational receptors.

To identify the detailed priority regions of concern, method of incorporating receptor population density into noncarcinogenic health risk assessment based on local land use map was developed and carried out. And, the results suggested the areas of A at each population density and the areas of B at high and moderate population density for As, and the high residential density area within A region for Hg, should be regarded as the priority regions of concern in XDD, respectively. It was concluded that the developed method was an improvement on previous study for an abundance of information about pollutant-pathway-receptor and the integrated mapping was to provide a simply and powerful visual tool for risk managers which make it possible to develop the hierarchical health risk management measures for the areas with different risk priorities.

**Acknowledgments** This study was financially supported by the National Natural Science Foundation of China (51178172, 51039001, and 51378190), the Project of Chinese Ministry of Education (113049A), and the Research Fund for the Program for Changjiang Scholars and Innovative Research Team in University (IRT-13R17).

## References

- Al Rmalli SW, Harrington CF, Ayub M, Haris PI (2005) A biomaterial based approach for arsenic removal from water. *J Environ Monit* 7(4):279–282
- Bourennane H, Douay F, Sterckeman T, Villanneau E, Ciesielski H, King D, Baize D (2010) Mapping of anthropogenic trace elements inputs in agricultural topsoil from Northern France using enrichment factors. *Geoderma* 157(3–4):165–174
- Cesari D, Contini D, Genga A, Siciliano M, Elefante C, Baglivi F, Daniele L (2012) Analysis of raw soils and their re-suspended PM10 fractions: characterisation of source profiles and enrichment factors. *Appl Geochem* 27(6):1238–1246
- Charlesworth S, De Miguel E, Ordóñez A (2011) A review of the distribution of particulate trace elements in urban terrestrial environments and its application to considerations of risk. *Environ Geochem Health* 33(2):103–123
- Chen H, Lu XW, Li LY (2014) Spatial distribution and risk assessment of metals in dust based on samples from nursery and primary schools of Xian, China. *Atmos Environ* 88:172–182
- Chen JQ, Wang ZX, Wu X, Zhu JJ, Zhou WB (2011) Source and hazard identification of heavy metals in soils of Changsha based on TIN model and direct exposure method. *T Nonferrous Metal Soc* 21(3):642–651
- Christoforidis A, Stamatis N (2009) Heavy metal contamination in street dust and roadside soil along the major national road in Kavala's region, Greece. *Geoderma* 151(3–4):257–263
- CNEMC (China National Environmental Monitoring Center) (1990) Background values of soil elements in China, 1st edn. Chinese Environmental Science Press, Beijing (in Chinese)
- Duker AA, Carranza EJM, Hale M (2005) Arsenic geochemistry and health. *Environ Int* 31(5):631–641
- Ferreira-Baptista L, De Miguel E (2005) Geochemistry and risk assessment of street dust in Luanda, Angola: a tropical urban environment. *Atmos Environ* 39(25):4501–4512

- Hu X, Zhang Y, Luo J, Wang T, Lian H, Ding Z (2011) Bioaccessibility and health risk of arsenic, mercury and other metals in urban street dusts from a mega-city, Nanjing, China. *Environ Pollut* 159(5): 1215–1221
- Hughes MF (2002) Arsenic toxicity and potential mechanisms of action. *Toxicol Lett* 133(1):1–16
- Jiang Y, Hu X, Yves UI, Zhan H, Wu Y (2014) Status, source and health risk assessment of polycyclic aromatic hydrocarbons in street dust of an industrial city, NW China. *Ecotoxicol Environ Saf* 106:11–18
- Kükrer S, Şeker S, Abaci ZT, Kutlu B (2014) Ecological risk assessment of heavy metals in surface sediments of northern littoral zone of Lake Çıldır, Ardahan, Turkey. *Environ Monit Assess* 186(6):3847–3857
- Kurt-Karakus PB (2012) Determination of heavy metals in indoor dust from Istanbul, Turkey: estimation of the health risk. *Environ Int* 50: 47–55
- Li H, Qian X, Hu W, Wang Y, Gao H (2013) Chemical speciation and human health risk of trace metals in urban street dusts from a metropolitan city, Nanjing, SE China. *Sci Total Environ* 456–457: 212–221
- Li F, Huang JH, Zeng GM, Yuan XZ, Liang J, Wang XY (2012) Multimedia health risk assessment: a case study of scenario-uncertainty. *J Cent South Univ* 19(10):2901–2909
- Li ZW, Zeng GM, Zhang H, Yang B, Jiao S (2007) The integrated eco-environment assessment of the red soil hilly region based on GIS—a case study in Changsha City, China. *Ecol Model* 202(3–4):540–546
- Liu E, Yan T, Birch G, Zhu Y (2014a) Pollution and health risk of potentially toxic metals in urban road dust in Nanjing, a mega-city of China. *Sci Total Environ* 476–477:522–531
- Liu M, Yang Y, Yun X, Zhang M, Li QX, Wang J (2014b) Distribution and ecological assessment of heavy metals in surface sediments of the East Lake, China. *Ecotoxicology* 23(1):92–101
- Lu X, Wang L, Li LY, Lei K, Huang L, Kang D (2010) Multivariate statistical analysis of heavy metals in street dust of Baoji, NW China. *J Hazard Mater* 173(1–3):744–749
- Luo XS, Yu S, Li XD (2011) Distribution, availability, and sources of trace metals in different particle size fractions of urban soils in Hong Kong: implications for assessing the risk to human health. *Environ Pollut* 159(5):1317–1326
- Mandal BK, Suzuki KT (2002) Arsenic round the world: a review. *Talanta* 58(1):201–235
- MEPPRC (2014) Technical guidelines for risk assessment of contaminated sites (HJ 25.3–2014). Ministry of Environmental Protection of the People's Republic of China, Beijing (in Chinese)
- National Environmental Protection Agency of China (1995) Environmental Quality Standard for Soils (GB 15618–1995). China Environmental Science Press, Beijing (in Chinese)
- Nelson DW, Sommers LE (1982) Total carbon, organic carbon and organic matter. In: Page AL, Miller RH, Keeny DR (eds) *Methods of soil analysis, part 2, chemical and microbiological properties*, 2nd edn. American Society of Agronomy, Inc. Madison
- Nyamangara J (1998) Use of sequential extraction to evaluate zinc and copper in a soil amended with sewage sludge and inorganic metal salts. *Agr Ecosyst Environ* 69(2):135–141
- Pan YM, Yang GZ (1988) Hunan soil background values and research methods. Chinese Environmental Science Press, Beijing (in Chinese)
- Pandey B, Agrawal M, Singh S (2014) Coal mining activities change plant community structure due to air pollution and soil degradation. *Ecotoxicology* 23(8):1474–1483
- Peña-Fernández A, González-Muñoz MJ, Lobo-Bedmar MC (2014) Establishing the importance of human health risk assessment for metals and metalloids in urban environments. *Environ Int* 72:176–185
- Saeedi M, Li LY, Salmanzadeh M (2012) Heavy metals and polycyclic aromatic hydrocarbons: pollution and ecological risk assessment in street dust of Tehran. *J Hazard Mater* 227–228:9–17
- Shi G, Chen Z, Bi C, Li Y, Teng J, Wang L, Xu S (2010) Comprehensive assessment of toxic metals in urban and suburban street deposited sediments (SDSs) in the biggest metropolitan area of China. *Environ Pollut* 158(3):694–703
- Sutherland RA (2000) Bed sediment-associated trace metals in an urban stream, Oahu, Hawaii. *Environ Geol* 39(6):611–627
- Tang R, Ma K, Zhang Y, Mao Q (2013) The spatial characteristics and pollution levels of metals in urban street dust of Beijing, China. *Appl Geochem* 35:88–98
- USEPA (1996) Soil screening guidance: technical background document (EPA/540/R-95/128). US Environmental Protection Agency, Washington DC
- USEPA (2001) Supplemental guidance for developing soil screening levels for superfund sites (OSWER 9355.4-24). US Environmental Protection Agency, Washington DC
- US Department of Energy (2004) RAIS: risk assessment information system. US Department of Energy, Washington DC
- Van den Berg R (1995) Human exposure to soil contamination: a qualitative and quantitative analysis towards proposals for human toxicological intervention values. Algemeen Vertaalebureau Muiderkring, Netherlands
- Walcek C, De Santis S, Gentile T (2003) Preparation of mercury emissions inventory for eastern North America. *Environ Pollut* 123(3): 375–381
- Wei BG, Yang LS (2010) A review of heavy metal contaminations in urban soils, urban road dusts and agricultural soils from China. *Microchem J* 94(2):99–107
- Yang B, Chen Z, Zhang C, Dong J, Peng X (2012) Distribution patterns and major sources of dioxins in soils of the Changsha-Zhuzhou-Xiangtan urban agglomeration, China. *Ecotoxicol Environ Saf* 84: 63–69
- Ye X, Qian H, Xu P, Zhu L, Longnecker MP, Fu H (2009) Nephrotoxicity, neurotoxicity, and mercury exposure among children with and without dental amalgam fillings. *Int J Hyg Environ Health* 212(4):378–386
- Yu BB, Wang Y, Zhou QX (2014) Human health risk assessment based on toxicity characteristic leaching procedure and simple bioaccessibility extraction test of toxic metals in urban street dust of Tianjin, China. *PLoS One* 9(3):e92459
- Zhang J, Deng H, Wang D, Chen Z, Xu S (2013) Toxic heavy metal contamination and risk assessment of street dust in small towns of Shanghai suburban area, China. *Environ Sci Pollut Res* 20(1):323–332
- Zhao H, Li X (2013) Understanding the relationship between heavy metals inroad-deposited sediments and washoff particles in urban stormwater using simulated rainfall. *J Hazard Mater* 246–247:267–276
- Zheng N, Liu J, Wang Q, Liang Z (2010) Health risk assessment of heavy metal exposure to street dust in the zinc smelting district, Northeast of China. *Sci Total Environ* 408(4):726–733
- Zhou T, Xi CZ, Dai TG, Huang DY (2008) Comprehensive assessment of urban geological environment in Changsha City. *Guangdong Trace Elem Sci* 15(6):32–38 (in Chinese)
- Zoller WH, Gladney ES, Duce RA (1974) Atmospheric concentrations and sources of trace metals at the South Pole. *Science* 183(4121): 198–200